

ORIGINAL RESEARCH ARTICLE

Adsorption of Cu (II) ions from aquatic environment using pre-irradiated Ethylene Tetrafluoroethylene Film

Shahnaz Sultana^{1,*}, S. M. Mobin Sikder², Nazia Rahman¹, MD. Nabul Sardar¹, Sapan Kumar Sen³, Shakila Satter Rini², Mim Mostakima Mila²

¹ Nuclear and Radiation Chemistry Division, Institute of Nuclear Science and Technology, Atomic Energy Research Establishment, Bangladesh Atomic Energy Commission, Dhaka 1349, Bangladesh

² Chemistry Department, Jahangirnagar University, Savar, Dhaka 1342, Bangladesh

³ Institute of Electronics, Atomic Energy Research Establishment, Bangladesh Atomic Energy Commission, Dhaka 1349, Bangladesh

* Corresponding author: Shahnaz Sultana, shahnazju32@gmail.com

ABSTRACT

Although copper (Cu) is a very beneficial metal, having too much of it in the body can cause lung issues, severe anemia, nausea, and vomiting. In order to extract Cu (II) ions from aqueous solution, an adsorbent was constructed in this study employing pre-irradiation grafted Ethylene tetrafluoroethylene (ETFE) film. The grafting method was used to binary monomers of sodium styrene sulfonate (SSS) and acrylic acid (AA), where NaCl served as an additive. The grafted polymer was also subjected to studies of tensile strength, water uptake, surface area extension, Scanning Electron Microscopy (SEM), and Fourier Transform Infrared spectroscopy (FTIR). The adsorption of Cu (II) was investigated with respect to pH, starting metal ion concentrations, contact time, monomer concentrations, and temperature. With 50 kGy of radiation dose, 4% NaCl, and 30% of monomer solution (SSS:AA = 1:2) in water generated the highest graft yield of 470%. The maximum adsorption capacity (412 mg g^{-1}) was discovered with an initial concentration of 2500 mg L^{-1} , a pH of 4.86, and a contact time of 24 h at room temperature ($25 \text{ }^\circ\text{C}$). A monolayer adsorption was recommended by the good linking between experimental data and the Langmuir Isotherm Model. The kinetic adsorption data closely fitted with the pseudo-second-order reaction. Due to its increased adsorption capacity and reusability, the synthesized new grafted polymer can be considered an efficient adsorbent for Cu (II) removal from wastewater.

Keywords: Cu (II); adsorption capacity; Ethylene Tetrafluoroethylene Film; Fourier Transform Infrared spectroscopy; reusability

ARTICLE INFO

Received: 11 June 2023
Accepted: 10 August 2023
Available online: 4 January 2024

COPYRIGHT

Copyright © 2024 by author(s).
Applied Chemical Engineering is published by EnPress Publisher, LLC. This work is licensed under the Creative Commons Attribution-NonCommercial 4.0 International License (CC BY-NC 4.0).
<https://creativecommons.org/licenses/by-nc/4.0/>

1. Introduction

One of the most serious environmental issues is the presence of heavy metals in water systems^[1]. They are non-biodegradable and extremely poisonous, and they can harm aquatic life and the quality of water supplies. These substances can accumulate through the food chain even in low amounts, affecting animals, plants, and ultimately human health. One of these substances, such as copper, can be harmful to human health when present in excess. This metal is widely dispersed because it is introduced into the environment both naturally and mostly through human activities. The “Wilson disease” is brought on by an excess of copper in humans and can result in lung problems, acute anemia, nausea,

and vomiting. Additionally, it harms the kidneys and causes coma, stomach, and intestinal distress^[2]. According to the World Health Organization (WHO), 2 mg L⁻¹ is the maximum concentration of Cu (II) that should be present in drinking water^[3]. They are not only harmful to humans, but they can also seriously harm the aquatic ecosystem. Thus, efficient Cu (II) recovery from aqueous solution and sea water is crucial for safeguarding both humans and the ecosystem's biodiversity. To remove heavy metals from an aqueous solution, a number of treatment strategies, including solvent extraction, ion exchange, adsorption, and precipitation have been proposed and used^[4-6]. The most well-liked technology among these is adsorption^[7].

Numerous ligands have been researched to date, including imidazole, thiocarbamate amidoxime, and phosphoryl groups^[8,9]. These organic ligands improve the capacity and selectivity of adsorption for metal ions that are chemically or firmly bound to adsorbents. In addition to these ligands, solid carriers are essential components of adsorbents since they must completely sustain adverse conditions such as high pH, temperature, and radiation dose. These polymers should also have adequate surface area and structure to allow for covalent connections between active groups on their structures. Graft polymer has recently emerged as a significant asset in the area of heavy metal removal from aqueous solutions^[10]. Because the adsorbent in this situation has a higher adsorption capacity and can be reused, the possibility of secondary pollution is decreased. This process involves attaching the functional monomers to the parent polymer chain via covalent bonds. This procedure is the most effective because it enables the grafted monomer to perform a variety of activities on the parent polymer without affecting the parent polymer's mechanical properties^[11]. The broad penetration of the polymer chain and the quick and uniform production of radicals make the radiation-induced grafting approach favorable^[12].

Various materials, including polyethylene (PE), polypropylene (PP), Polyethylene terephthalate (PET), Polytetrafluoroethylene (PTFE), graphene oxide, natural polymers, etc., were utilized in the past as parent polymers^[13-15]. Due to its mechanical qualities, Ethylene tetrafluoroethylene (ETFE) film, which was used as the mother polymer in the current experiment, is primarily used in the nuclear and aerospace industries for cable wraps and wire coatings. In this study, acrylic acid and sodium styrene sulfonate were used as monomers where NaCl acted as an additive to Ethylene tetrafluoroethylene. Previously, the same monomers were utilized without the addition of any additives, while ETFE was exposed to electron accelerator radiation and used as a cation exchange membrane after being grafted^[16].

To determine whether the Ethylene tetrafluoroethylene (ETFE) film could be used as an adsorbent, the film was first characterized using Fourier Transform Infrared spectroscopy, Scanning Electron Microscopy, and tensile strength. Later, the adsorption capacity was assessed under a variety of conditions of pH, contact time, copper concentrations, monomer concentrations, and temperature. Adsorption isotherms were investigated to clarify the likely adsorption mechanism and to provide information regarding maximum sorption capacity, sorption energy, homogeneity/heterogeneity, and affinity between sorbent and adsorbent that might help in understanding the process taking place.

2. Experimental

2.1. Materials and methods

The base polymer, ETFE was collected from Sigma Aldrich, USA. Two monomers, AA and SSS were also purchased from Sigma Aldrich, USA. NaOH, NaCl, HCl, and Cu (II) sulfate were supplied by Merck, Germany. All glassware used in this experiment was cleaned properly at room temperature and dried in an oven at 60 °C. In this case, distilled deionized (DDI) water was used for both washing and preparing the solution. pH, EC, and TDS

values of the DDI water were 6.7, 0.2 μS , and 0.1 mg L^{-1} respectively. **Table S1** (Supplementary materials) displays some of the mother polymer's fundamental characteristics.

2.2. Instruments and apparatus

The Co (60) gamma-irradiator from the Institute of Food and Radiation Biology, Atomic Energy Research Establishment, Savar, Dhaka, Bangladesh, was used to regulate the dose rate during the synthesis of the graft copolymer. It was a 90 kCi batch-type panoramic irradiator with a dosage rate of 13.7 kGy h^{-1} that was collected from BRIT, India. Utilizing IRPrestige21 from Shimadzu Corporation, Japan, investigation of FTIR-ATR in the wavenumber range of $700\text{--}4000 \text{ cm}^{-1}$ was accomplished. Scanning Electron Microscopy was used to measure the change of surface morphology after grafting, the model used in this study was JSM-6490 LA, JEOL. The concentrations of Cu (II) ion of different solutions were analyzed by UV-VIS Spectrophotometer (Model: UV2401PC from Shimadzu, Japan). Mechanical Stability was determined by a Universal Testing Machine Testometric, model M 500-100CT, UK. During this experiment, the crosshead speed was 2 mm/min, gauge length was 20 mm, and load range was 250 N.

2.3. Preparation of sulfonated ETFE adsorbent

Figure 1 shows the newly developed polymeric adsorbent's preparation procedure. The ETFE strips were cut into pieces sized 2.5 cm by 4 cm, cleaned in DDI water and acetone, dried in a vacuum oven at $50 \text{ }^\circ\text{C}$, and weighed (W_0). The monomer solutions were all made by combining SSS and AA in a 1:2 (SSS:AA) ratio. By mixing 4% NaCl solution in DDI water with various SSS and AA compositions, several combinations, including 9%, 13.5%, 15%, 18%, 24%, and 30%, were created. The Cobalt-60 (^{60}Co) irradiator was used to apply a 50 kGy dose of gamma radiation to polymer strips. In contrast, even after several weeks and at high temperature, the ETFE films in the monomer solution remained unchanged without the pre-irradiation. The irradiation films were then quickly maintained under dry ice conditions. In the meantime, argon gas was bubbled in gas-washing bottles containing monomer solutions for 40 min at room temperature. Following that, each of the two irradiated films was placed into a 25 mL airtight vial with a bubbled mixture as soon as possible to prevent the oxidation of the air. After that, the grafting reaction was allowed to complete for 5 h in a water bath at $80 \text{ }^\circ\text{C}$. After being washed many times to get rid of homopolymers and unreacted monomers, the films were ready to be used as adsorbents. The ETFE-g-SSS-AA strips were weighed (W_1) after being dried in the vacuum oven at $50 \text{ }^\circ\text{C}$. The grafting yield (GY) of the grafted ETFE adsorbent was calculated gravimetrically as Equation (1):

$$GY = \frac{W_1 - W_0}{W_0} \times 100 \quad (1)$$

The method became simpler by the fact that no inhibitor was added during the grafting process and the adsorbent didn't need to be treated. Moreover, by appropriately varying the irradiation and reaction parameters, the amount of the grafted moiety can be managed. **Figure 1** depicts a flowchart diagram showing how grafted ETFE film was prepared.

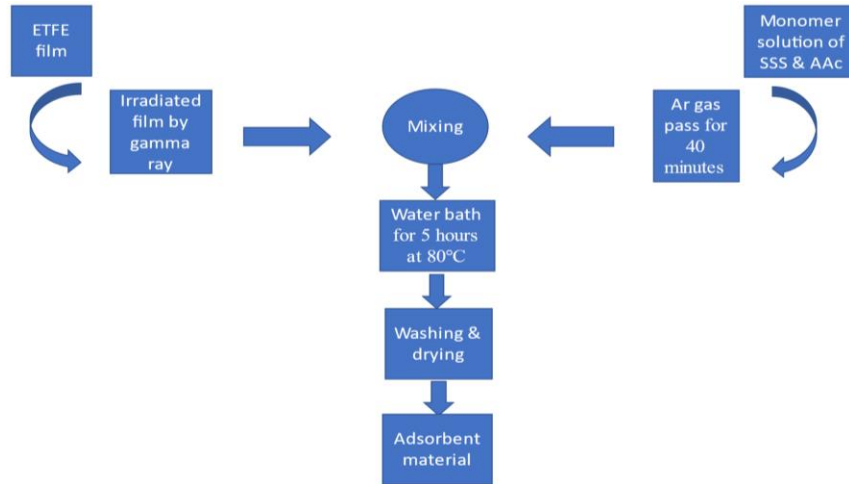


Figure 1. Flow chart diagram of the preparation of ETFE-g-AA-SSS film.

2.4. Characteristics

2.4.1. Thickness (mm) and Surface area extension (%)

The thickness and surface area changed after grafting. Surface Area Extension (%) was calculated by the following Equation (2):

$$\text{Surface Area Extension (\%)} = \frac{S_1 - S_0}{S_0} \times 100 \quad (2)$$

where, S_1 and S_0 are the surface areas of the grafted and pure films respectively which were calculated by measuring the length, width, and height with the slide calipers.

2.4.2. Water uptake (%)

By immersing the grafted film in 40 mL of DDI water at 60 °C for one hour, water uptake was monitored. After that, a soft tissue was used to carefully remove the weight of the wet layer from the surface water. Water Uptake was measured gravimetrically by the following Equation (3):

$$\text{Water uptake (\%)} = \frac{W_w - W_d}{W_w} \times 100 \quad (3)$$

where, W_w and W_d are the weights of the wet film and dry film respectively.

2.4.3. Tensile strength

Tensile properties of different films were measured using Universal Testing Machine (Testometric, model M 500-100CT, UK). The crosshead speed and gauge length used were 2 mm/min and 20 mm respectively with load range 250 N throughout the experiment. The adsorbents were cut into 2 cm vs 14 cm pieces to measure mechanical property. Tensile strengths were measured after water uptake. After radiation grafting the flexibility of the film increased causing decrease of tensile strength. The rigidity of the produced membranes reduced as grafting yield, volume, and surface area increased.

2.4.4. Adsorption capacity (q)

The total metal ion adsorption capacity (q) of the synthesized copolymer for Cu cations was calculated using the following Equation (4):

$$q = V \times \left(\frac{C_1 - C_2}{C_1} \right) \times W \quad (4)$$

where,

q is the adsorption capacity (mg g^{-1} of adsorbent),
 W is the weight of the grafted PE film (g),
 V is the volume of Cu solution (L),
 C_1 and C_2 are the concentrations (mgL^{-1}) of the metal ions before and after adsorption.

2.4.5. Regeneration and reuse study

The adsorbent can be regenerated after adsorption by desorption with certain solvents. Regeneration efficiency (%) can be calculated by the following Equation (5):

$$\text{Regeneration efficiency (\%)} = \frac{\text{uptake of metal ion in the second cycle}}{\text{uptake of metal ion in the first cycle}} \times 100 \quad (5)$$

2.5. Preparation of Cu solution for UV measurement

Cu concentration was measured by the spectrophotometric method by preparing standard solutions with known Cu concentrations to create a calibration curve. Then, the absorbance of the standard solutions at a specific wavelength was measured using the spectrophotometer. Cu (II) stock solution was made using DDI water, and the required Cu (II) solution concentrations were made by properly diluting the stock solutions. Wavelengths of 530 nm and 820 nm were used to determine low and high concentrations of Cu (II) respectively by using UV-Vis spectrophotometer from Cu (II) aqueous solutions.

3. Results and discussion

3.1. Physico-chemical properties of the grafted ETFE films

After grafting, the physicochemical characteristics of the ETFE films underwent a transformation. **Table S2** (Supplementary materials) shows several physicochemical characteristics of the grafted ETFE film. Despite a decline in tensile strength, the extent of grafting, surface area extension, and water uptake increased dramatically. The degree of grafting grew rapidly from 4.5% to 470% and the surface area extension also showed the same trend from 0.15% to 60% with the monomer concentration of 9% to 30% in water. The thickness rose significantly from 0.025 mm (pure ETFE) to 0.028 mm (470% grafted ETFE). Water Uptake also rose from 0.44% to 210.62% with monomer solutions because of the increase of the swollen property due to the additional hydrophilic sites. These findings are consistent with those reported in the prior research^[17,18]. However, as the degree of grafting increased, the tensile strength decreased from 65 MPa (at 4.5% GY) to 60 MPa (at 190% GY), indicating that the prepared adsorbents became more flexible in general.

3.2. FTIR analysis

PerkinElmer spectrum two FT-IR spectrophotometer was used to characterize the structural properties of the grafted films with both before and after Cu adsorption, as well as bare ETFE film showed in **Figure 2**. In spectrum (a), the ETFE film spectra showed a number of strong bands in the 1000 cm^{-1} – 1300 cm^{-1} range that resembled the C–F of CF_2 groups^[19]. When comparing the spectra (a) with (b), it could be seen that the –OH stretching vibrations of AA exhibited a broad absorption peak between 3200 and 3600 cm^{-1} . The C=O groups of AA corresponded to the absorption peak at 1718 cm^{-1} . The characteristic peak of a substituent linked to the para-position of the benzene ring is the absorption peak at 842 cm^{-1} . The peak at 1020 cm^{-1} was due to a symmetrical stretching vibration of S=O and 1168 cm^{-1} for antisymmetric^[20,21]. All these new adsorption peaks showed that AA and SSS had been successfully grafted onto the ETFE film. Comparing the spectrum (b) with (c), the peak at 1718 cm^{-1} for C=O

groups of AA became sharper. Another change happened at 1025 cm^{-1} , which increased and represented the S=O groups of SSS indicating Cu adsorption.

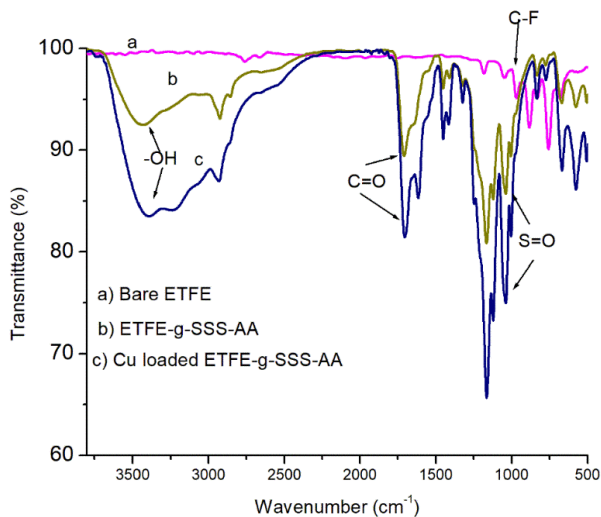


Figure 2. FTIR spectrum (a) bare ETFE, (b) ETFE-g-SSS-AA film and (c) Cu Loaded ETFE-g-SSS-AA film.

3.3. SEM analysis

The Scanning Electron Microscopy of the membranes was examined using VEGA3 TESCAN located in IE, AERE, BAEC. **Figure 3** shows the surface morphologies observed by SEM of raw ETFE (**Figure 3a,c**) and ETFE-g-SSS-AA film (**Figure 3b,d**). The surface nature of the ETFE sample remained almost similar after grafting, according to the microscopic appearance of the SEM image. Raw ETFE film had a thick, continuous, homogenous, smooth surface similar to that of the majority of semi-crystalline polymers, including LDPE, PP, etc.^[22]. After the grafting reaction, the constitution of ETFE changed and the surface showed little change with few spots of various-sized grafted pieces, which could be due to the softness of the ETFE^[23].

This can be noted that the grafting of SSS and AA onto PE to a great extent is homogeneous as the distribution and concentration of the grafting particles on the surface are analogous. The Energy dispersive X-ray spectrum for Cu (II) loaded adsorbent exhibits the peak for Cu in **Figure 3e**. A table in **Figure 3e** represents the elemental analysis of Cu-loaded ETFE-g-SSS-AA which shows a chemical composition of 73.6% C, 20.09% F, and 5.5% Cu. After Cu (II) adsorption process, the characteristic peaks, and the percentage (in mass) of Cu were clearly proved to be the adsorption of Cu.

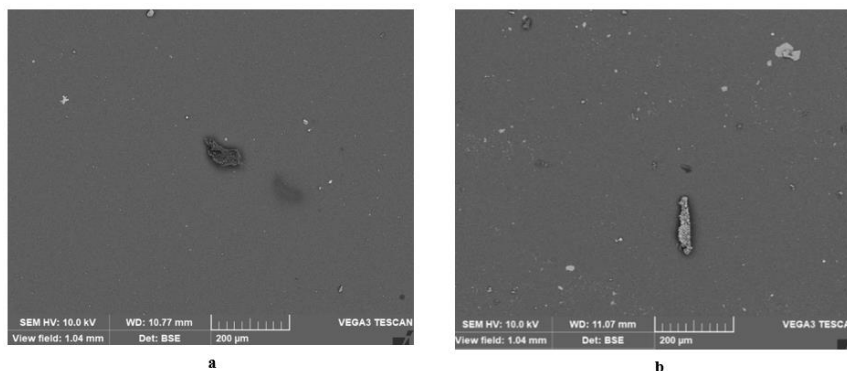


Figure 3. (Continued).

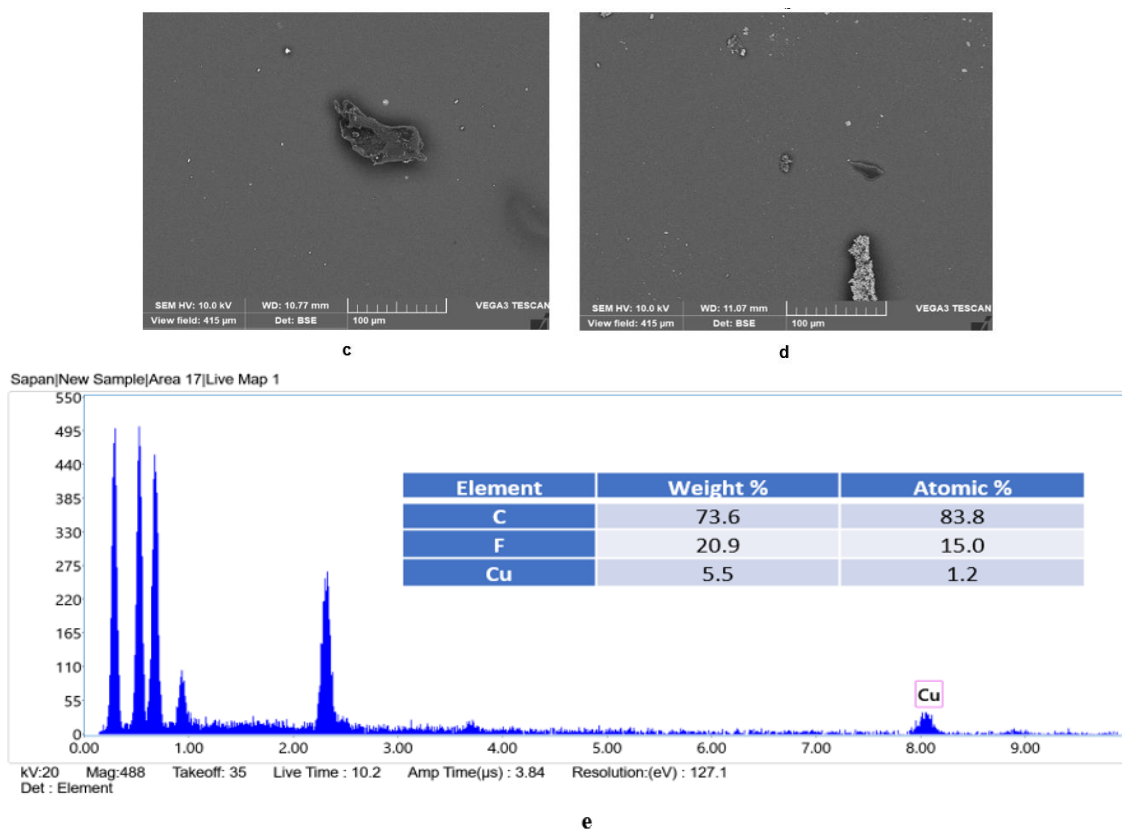


Figure 3. SEM images of bare ETFE film [(a) 200 times magnification and (c) 500 times magnification], ETFE-g-SSS-AA film [(b) 200 times magnification and (d) 500 times magnification], and (e) the corresponding Energy dispersive X-ray spectrum (EDX) with elemental composition of ETFE-g-SSS-AA film after Cu (II) adsorption.

3.4. Studies of monomer concentrations on GY

Monomer concentrations played an important role in GY because GY increased significantly with increasing the concentrations of monomer solution graphically as presented in **Figure 4a**. The monomer concentrations were kept 1:2 for SSS:AA in water for all solutions. The concentrations varied from 9% (3% SSS and 6% AA in water) to 30% (10% SSS and 20% AA in water) where 4% NaCl was used as an additive. Initially, GY showed very little change from 4.5% to 12.5% with the monomer concentration of 9% to 12%, however; after that, it increased sharply to the highest point of 470% at the mixture of 10% SSS and 20% AA in water.

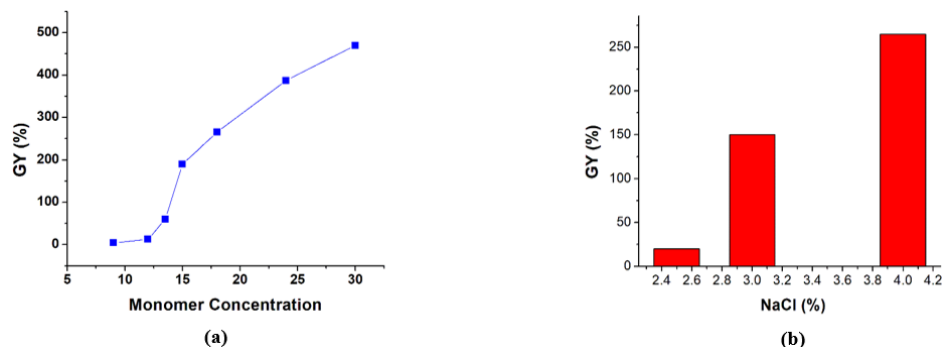


Figure 4. (Continued).

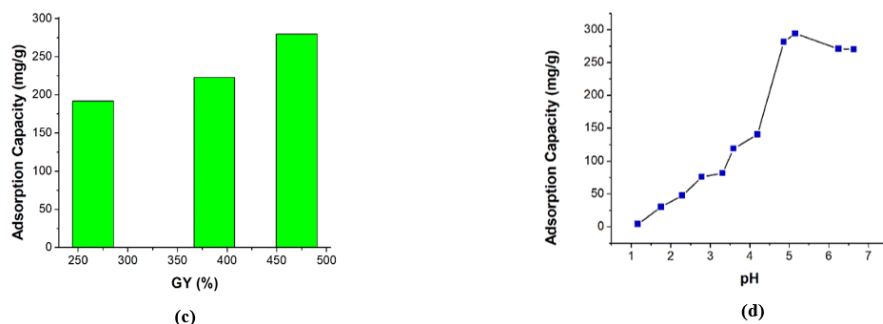


Figure 4. (a) Influence of monomer concentration on GY; (b) Influence of NaCl on GY; (c) The effect of GY on the adsorption capacity (pH: 4.86, temperature: 25 °C, conc: 1000 mg/L); (d) The effect of pH on the adsorption capacity (temperature: 25 °C, radiation dose: 50 kGy, conc: 1000 mg/L).

3.5. Addition of NaCl into monomer solution

Addition of NaCl promoted the GY of the adsorbent. At below 4% NaCl the percentage of GY attained is very low. Even GY was only 20% when 2.5% NaCl was added into the monomer solution as shown in **Figure 4b**. Thus, the addition of NaCl is greatly important to the formation of the high-capacity adsorbent. In this study, 4% NaCl was used as an optimum amount.

3.6. Adsorption capacity vs GY

Higher GY promoted the percentage of Cu (II) uptake represented in **Figure 4c** (pH: 4.86, vol: 10 mL, radiation dose: 50 kGy, conc: 1000 mg/L). The percentage of Cu (II) uptake increased as the percentage of GY increased. Because there are more functional groups at higher GY levels, more Cu (II) can be captured there^[24,25]. The GY of 470% showed the highest q .

3.7. Effect of pH

In aqueous solution, pH influences Cu (II) adsorption significantly^[26]. **Figure 4d** illustrates the impact of pH on Cu (II) adsorption of PE-g-SSS-AA films (GY: 470%, vol: 10 mL, radiation dose: 50 kGy). Firstly, q increased quickly from 4.04 to 281 mg g⁻¹ with pH 1.17 to 4.86 and reached the highest point (294.33 mg g⁻¹) at pH 5.15. After that, q dropped slowly by 268 mg g⁻¹ at pH 6.68. The trend was remarkably similar to other investigations of Cu removal, such as using biosorbents made from the hulls of Indian jujube seeds^[27]. By preparing acidic and basic media with HCl and NaOH, respectively, the pH of the solution was adjusted. The grafted ETFE films displayed decreased ability to chelate copper ions at low pH. As pH increased, the sulfonic group deprotonated, resulting in active sites that created complexes with Cu (II) ions. Thus, it showed the highest adsorption capacity at pH 5.35. However, when pH further increased, NaOH in Cu (II) solution also increased. Cu (II) ions showed more affinity towards (OH⁻) ions and form Cu(OH)₂ precipitation. Thus, at higher pH levels adsorbents had lower capacity for Cu (II) adsorption^[28]. The mother solution had a pH of 4.86 and included 271.5 mg g⁻¹ of q from a 1000 mg L⁻¹ Cu solution. The maximum value of q , 294.33 mg g⁻¹ at pH 5.15, was close to the value of q at pH 4.86. Moreover, q gradually decreased after pH 5.15. Therefore, pH was kept unchanged to avoid protonation and precipitation of Cu (II) for other adsorption tests in this experiment.

3.8. Effect of contact time

Plotting the ETFE-g-SSS-AA adsorption capacity vs contact time (h) under specific conditions (GY: 470%, initial metal ion concentration: 20 mg/L, pH: 4.86, vol: 10 mL, radiation dose: 50 kGy) is shown in **Figure 5a**. The range of interaction time was set at 0.5 h to 30 h. The adsorption occurred swiftly at the initial stages up to 4.5 h and became slower near the equilibrium. There was no considerable change in the q of the adsorbent after

equilibrium (24 h). Up to 30 h, all metals were investigated. After 24 h the equilibrium adsorption for Cu (II) was achieved at 11.46 mg g⁻¹.

3.9. Kinetic modeling

To investigate the kinetic mechanism of adsorption, two different kinetic models pseudo-first-order (PFO) and pseudo-second-order (PSO) kinetic models are used^[29]. The PFO and PSO are described by the following Equations (6) and (7):

$$\text{Log} (Q_e - Qt) = -\left(\frac{k_1}{2.303}\right)t + \text{Log} Q_e \quad (6)$$

$$\frac{t}{Qt} = \frac{1}{(k_2 Q_e)^2} + t/Q_e \quad (7)$$

where,

Q_e (mg g⁻¹) is the adsorption capacity at equilibrium,

Qt (mg g⁻¹) is the adsorption capacity at time t (h),

k_1 (h⁻¹) and k_2 (g mg⁻¹ h⁻¹) are the first and second-order kinetic constants, respectively.

3.9.1. Pseudo-first-order kinetic model (PFO)

The graph of log (Q_e-Q_t) vs. time has been used to calculate the pseudo-first-order rate constant (**Figure 5b**). The slope and intercept of the trend line can be employed to determine the values of k_1 and Q_e . It can be concluded that the experimental Q_e (11.46 mg g⁻¹) value and Q_e (7.35 mg g⁻¹) values measured from the 1st-order kinetic model are different from each other. The correlation between experimental data and PFO kinetic model data was presented by correlation coefficient (R^2). The values of k_1 , and R^2 for Cu (II) uptake were presented in **Table 1**.

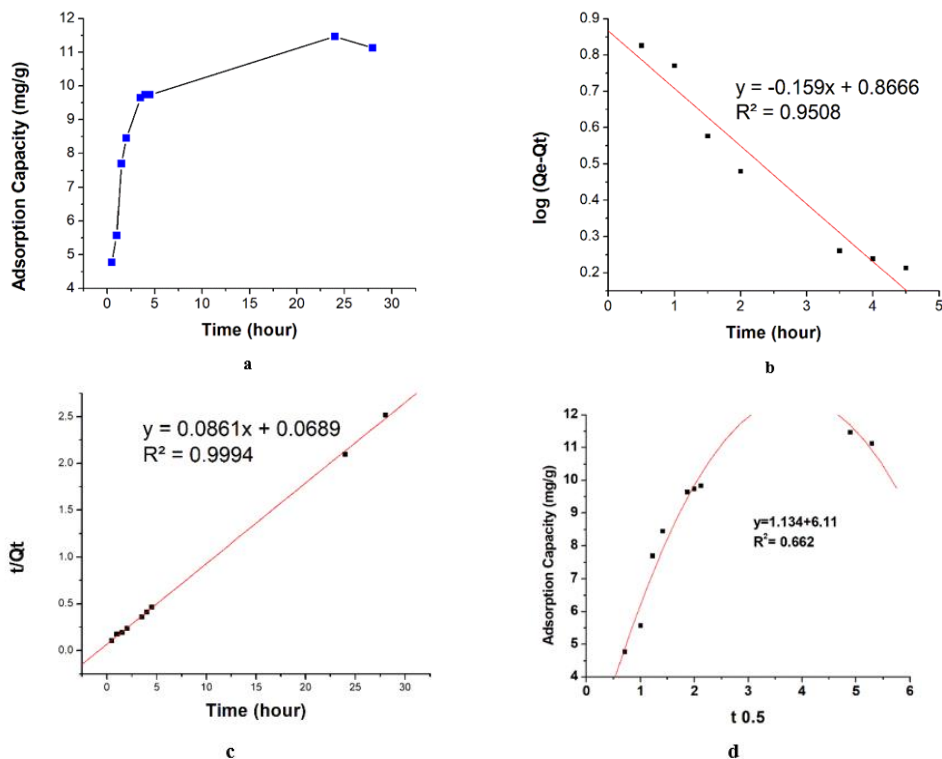


Figure 5. (a) Adsorption capacity varies with contact time at room temperature (2.5 °C), GY 4.7.0%, and pH 4.8.6, concentration 2.0. mg/L. Adsorption kinetics: (b) Pseudo-first-order kinetic model (c) Pseudo-second-order kinetic model and (d) Intraparticle diffusion model.

3.9.2. Pseudo-second-order kinetic model (PSO)

As could be seen from **Figure 5c**, t/Qt against time shows a linear relationship. The value of Q_e (mg g^{-1}) and k_2 ($\text{g mg}^{-1} \text{h}^{-1}$) are determined from the slope and intercept of the plot, respectively and they are summarized in **Table 1**. From the graph, it can be seen that the experimental Q_e value (11.46 mg g^{-1}) and the Q_e values (11.61 mg g^{-1}) calculated from the 2nd order kinetic model are very similar to each other. Moreover, the correlation coefficient value (R^2) was also very close to unity which further supports PSO kinetic model in the present experiment. Hence, the PSO kinetic model is suitable to understand Cu (II) uptake.

3.9.3. Intra-particle diffusion (IPD)

As the adsorption follows the PSO model the adsorption process might have been controlled by the intra-particle diffusion (IPD)^[30]. To get more extent of adsorption, the IPD plays an important role and it can be expressed as Equation (8):

$$qt = k_i t^{0.5} + C \quad (8)$$

where,

k_i is the intraparticle diffusion constant ($\text{mg g}^{-1} \text{h}^{-1}$) and

C is the intercept (reflects the boundary layer effect).

The figure will be linear if intraparticle diffusion plays a part in the adsorption process, and if these lines cross the origin, intraparticle diffusion is the rate-regulating step. The k_i value can be calculated from the slope of the plot (**Figure 5d**) and is presented in **Table 1**. The plot of q versus $t^{0.5}$ does not pass through the origin. This indicates that intra-particle diffusion is not the only rate controlling step, moreover, there are other kinetic models that may control the adsorption rate^[31].

Table 1. The pseudo-first-order (PFO), pseudo-second-order (PSO) and intraparticle diffusion (IPD) kinetic models for Cu (II) uptake where the experimental value of q (Q_e) is 11.46 mg g^{-1} .

| PFO model | | | PSO model | | IPD model | | |
|------------------------------|---------------------------|--------|------------------------------|--|-----------|--|--------|
| Q_e (mg g^{-1}) | k_1 (h^{-1}) | R^2 | Q_e (mg g^{-1}) | k_2 ($\text{g mg}^{-1} \text{h}^{-1}$) | R^2 | k_i ($\text{mg g}^{-1} \text{h}^{-1}$) | R^2 |
| 7.3500 | 0.3662 | 0.9508 | 11.6144 | 0.1087 | 0.999 | 1.1340 | 0.6620 |

3.10. Temperature study

Temperature plays an important role in the adsorption capacity of the adsorbent. The adsorption capacity was studied with different temperatures of $8.3 \text{ }^\circ\text{C}$, $25 \text{ }^\circ\text{C}$, $60 \text{ }^\circ\text{C}$, $80 \text{ }^\circ\text{C}$, and $100 \text{ }^\circ\text{C}$ of 200 mg L^{-1} Cu (II) solution of unmodified pH. Adsorption capacity enhances with increasing temperature (4 h of heating period at different temperatures) as in **Figure 6a**. Adsorption capacity was found 125 mg g^{-1} at $8.3 \text{ }^\circ\text{C}$ but it raised 235 mg g^{-1} at $100 \text{ }^\circ\text{C}$ indicating that the sorption obeys endothermic manners.

3.11. Concentration study

The relationship between the initial concentration of metal ions and adsorption capacity is shown in **Figure 6b** (GY: 470%, pH: 4.86, vol: 10 mL, radiation dose: 50 kGy). As the concentration of metal ions rises, correspondingly rises the adsorption capacity. The abundance of active sites on the adsorbent surface contributes to the high adsorption capacity at low concentrations. However, at high concentrations, the active sites are completely filled with Cu (II), and as a result, no more active sites are available for ion bonding. The adsorption capacity in this experiment, which had initial Cu (II) concentrations of 97 mg L^{-1} to 953 mg L^{-1} , climbed quickly from 105 mg g^{-1} to 356 mg g^{-1} before gradually reaching a plateau, is an example of this phenomenon. The highest

adsorption capacity for Cu (II) was found to be 412 mg g⁻¹ at 2500 mg L⁻¹ at equilibrium. Therefore, from the concentration study, it is seen that the ETFE-g-SSS-AA film can be used to purify water from wastewater having less or a lot of Cu (II) contamination.

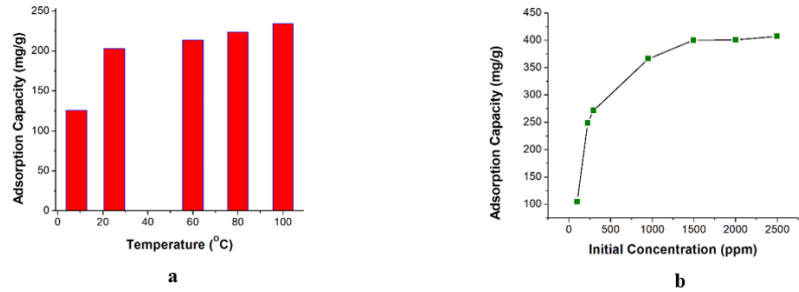


Figure 6. (a) Effect of temperature (pH: 4.86, GY 470%, concentration 1000 mg/L) and (b) initial metal ion concentration on the adsorption capacity (pH: 4.86, GY 470%, temperature: 25 °C).

3.12. Adsorption isotherm studies

Both the Langmuir and the Freundlich adsorption isotherms have been used to assess the ETFE-g-SSS-AA's ability to adsorb Cu (II) ions. The Langmuir isotherm, a single layer, or monolayer is theoretical, while the Freundlich isotherm is empirical. The Langmuir adsorption is established by the following linear Equation (9) and the dimensionless separation factor, R_L is expressed by Equation (10):

$$\frac{C_e}{Q_e} = \frac{C_e}{Q_o} + \frac{1}{(Q_o b)} \quad (9)$$

$$R_L = \frac{1}{(1 + Q_o b)} \quad (10)$$

where,

- C_e (mg L⁻¹) = concentration of the metal ion at equilibrium,
- Q_e (mg g⁻¹) = capacity of the adsorption at equilibrium,
- Q_o (mg g⁻¹) = monolayer adsorption capacity,
- b (L mg⁻¹) = Langmuir adsorption constant.

The value of R_L is an important factor in Langmuir adsorption isotherm. If $R_L > 1$, the reaction would be unfavorable but if $0 < R_L < 1$, it would be favorable. On the other hand, if the R_L values are 1 and 0.00 they would be linear and irreversible respectively. Here, Q_o and b can be calculated from the slope and intercept of the plot of $\frac{C_e}{Q_e}$ vs. C_e . The linearity of the plot, Q_o value, R^2 , and R_L values revealed that the adsorption followed the Langmuir isotherm model showed in **Figure 7a**, and displayed in **Table 2**.

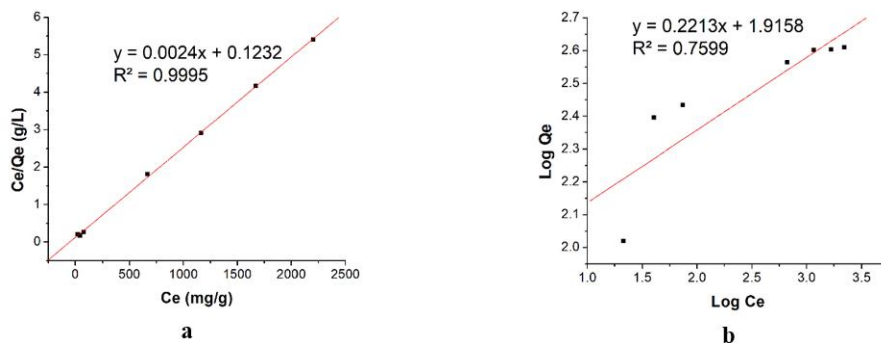


Figure 7. (a) Langmuir isotherms; (b) Freundlich isotherms.

Table 2: Isotherm parameters obtained from the adsorption study of Cu (II).

| Adsorption Isotherm Model | Parameters | Values |
|---------------------------|-----------------------------|--------|
| Langmuir | Q_0 (mg g ⁻¹) | 416.67 |
| | R_L | 0.11 |
| | R^2 | 0.99 |
| Freundlich | K_F (mg g ⁻¹) | 82.38 |
| | n | 4.51 |
| | R^2 | 0.76 |

On the other hand, the Freundlich isotherm can be expressed by the linear Equation (11), which demonstrates multilayer adsorption on heterogeneous surface:

$$\log Q_e = \ln K_f + \frac{1}{n} \log C_e \quad (11)$$

here,

Q_e = amount of Cu (II) adsorbed (mg g⁻¹) in equilibrium,

C_e = equilibrium concentration of Cu (II) solution (mg L⁻¹),

K_f and n = Freundlich constants which indicate the capacity and the intensity of the adsorption, respectively.

The values of K_f (mg g⁻¹) and n (L mg⁻¹) can be extracted by the intercept and slope of the plot of $\log Q_e$ vs. $\log C_e$ showed in **Figure 7b** and summarized in **Table 2**. The value of ‘n’ offers information about the favorability of the adsorption. Typically, ‘n’ values between 2 and 10 indicate favorable adsorption, while values between 1 and 2 suggest moderately challenging adsorption, and values below 1 indicate poor adsorption characteristics. The R^2 value was found 0.76 from this model indicating that the adsorption process is more compatible with the Langmuir adsorption isotherm model than the Freundlich isotherm model.

3.13. Probable reaction mechanism

It is likely that ETFE-g-SSS-AA films have both physical and chemical adsorption (functional groups) on their surface which may explain their high adsorption capability. Lone pair electrons can be provided by the “O” atoms in carboxyl and sulfonate groups to form a coordination bond with copper ions. **Figure 8** can be used to suggest one of the reaction mechanisms based on the findings of the kinetic model and isotherm model presented before. It should be noted that more probable reaction pathways may exist that may be liable for the adsorption.

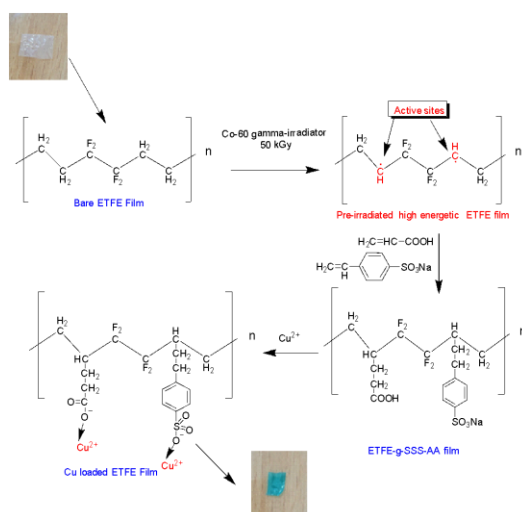


Figure 8. One of the simple reaction pathways of the formation of ETFE-g-SSS-AA adsorbent and interaction with Cu²⁺.

3.14. Regeneration and reuse study

The key to effectively reducing costs is reuse. The regeneration and reuse process of the metal-loaded adsorbents is significantly influenced by desorption. Desorption of the metal ions were carried out by 2M HCl, 2M HNO₃, 2M H₂SO₄, and 2M NaOH as eluting agents for 30 min. All the solvents responded to the regeneration process (**Figure S1**, Supplementary materials). However, the desorption rate was maximum for 2M HCl (99%).

At the same optimum operating conditions, the adsorption-desorption cycle was repeated. The adsorption capacity from the first cycle was 99 mg g⁻¹, while the second cycle's value was 71 mg g⁻¹. The findings indicate that this adsorbent is appropriate for further use.

Regeneration efficiency = 71%.

3.15. Cu (II) uptake capacity compared with other adsorbents

Earlier research in this area included numerous investigations where the removal capacities of the adsorbents ranged from poor to high. **Table 3** shows the comparison of Cu (II) uptake capacity of our prepared adsorbent with other adsorbents. In this study, the adsorbent capacity was found to be very high to remove Cu (II) from aqueous solution. The maximum adsorption capacity was found to be 412 mg g⁻¹, which was 2.14 times higher than that of the polypropylene fabric with the same functional groups^[32].

Table 3. Comparison of Cu (II) adsorption capacity of ETFE-g-SSS-AA film with some other adsorbents.

| S. no | Adsorbent | q (mg g ⁻¹) | Reference no |
|-------|--------------------------|-------------------------|---------------|
| 1 | Waste polypropylene (PP) | 192 | [32] |
| 2 | Activated neem bark | 21.78 | [33] |
| 3 | Lignite | 4.045 | [34] |
| 4 | Kaolinite | 10.78 | [35] |
| 5 | Chitosan | 53 | [36] |
| 6 | Activated red clay | 26.8 | [37] |
| 7 | Cashew nut shell | 20 | [38] |
| 8 | Grape seeds | 1.4 | [39] |
| 9 | HAp-coated-limestone/CS | 130.75 | [40] |
| 10 | HAP-coated-limestone | 90.90 | [41] |
| 11 | ZIF-8@GO | 482.29 | [42] |
| 12 | ETFE-g-SSS-AA | 412 | Present study |

4. Conclusion

By using the pre-irradiation process using NaCl as an additive, SSS and AA grafted ETFE adsorbent was successfully synthesized. FTIR, TGA, and SEM were used to characterize the produced adsorbent. 30% monomer solution (SSS:AA = 1:2) in water produced the highest graft yield of 470% with 50 kGy of radiation dose when 4% NaCl was added as an additive. The grafted polymer was examined using tensile strength, water uptake, and surface area extension. Cu (II) was absorbed from various aqueous solutions using the newly produced adsorbent. At an initial concentration of 2500 mg L⁻¹, a pH of 4.86, and a contact time of 24 h at room temperature (25 °C), the maximum adsorption capacity was found to be 412 mg g⁻¹ from the ETFE-g-SSS-AA of 470% GY. The strong agreement between experimental results and the Langmuir Isotherm Model pointed to monolayer adsorption. The pseudo-second-order process provided a good fit to the kinetic adsorption data. To sum up, the synthesized novel grafted polymer can be regarded as a good adsorbent for Cu (II) removal from wastewater due to its greater adsorption capacity and reusability.

Supplementary materials

Table S1: Properties of backbone polymer; **Table S2:** Functionalization degree of PET nanofibers at room temperature; **Figure S1:** Effect of solvents on desorption.

Author contributions

Conceptualization, SS and SMMS; methodology, SMMS; software, SS and SKS; validation, SMMS, SSR and MMM; formal analysis, SMMS and SS; investigation, NR and SS; resources, NR and SKS; data curation, SMMS, SSR and SS; writing—original draft preparation, SS; writing—review and editing, SMMS and SS; visualization, SMMS and SS; supervision, NR, MD, MNS and SS; project administration, NR; funding acquisition, SS. All authors have read and agreed to the published version of the manuscript.

Acknowledgments

The authors would like to express their gratitude to the International Atomic Energy Agency (IAEA) for their cooperation with the technical parts of this study. It is equally important to recognize the contributions made by the Institute of Food and Radiation Biology at Bangladesh Atomic Energy Research Establishment for providing irradiation facilities.

Conflict of interest

The authors declare no conflict of interest.

References

1. Mitra S, Chakraborty AJ, Tareq AM, et al. Impact of heavy metals on the environment and human health: Novel therapeutic insights to counter the toxicity. *Journal of King Saud University—Science* 2022; 34(3): 101865. doi: 10.1016/j.jksus.2022.101865
2. Benzaoui T, Selatnia A, Djabali D. Adsorption of copper (II) ions from aqueous solution using bottom ash of expired drugs incineration. *Adsorption Science & Technology* 2018; 36(1–2): 114–129. doi: 10.1177/0263617416685099
3. Sultana S, Ahmed FT, Rahman N, et al. Determination of Ni, Cu, Cd, Zn, Pb, Cr and Mn in some black and green tea leaves and their infusions available in Bangladeshi local markets. *Applied Chemical Engineering* 2023; 6(1): 28–37. doi: 10.24294/ace.v6i1.1940
4. Song Z, Huang W, Zhou Y, et al. Thermally regulated molybdate-based ionic liquids toward molecular oxygen activation for one-pot oxidative cascade catalysis. *Green Chemistry* 2020; 22(1): 103–109. doi: 10.1039/c9gc03646f
5. Deepa P, Pooja B, Ashok K, Pravin D. Adsorption of Cu (II) ions from aqueous solution by *A. Ficoidea*. *Journal of Advances and Scholarly Researches in Allied Education* 2018; 15(11): 203–208. doi: 10.29070/JASRAE.
6. Yuan L, Sun M, Liao X, et al. Solvent extraction of U (VI) by trioctylphosphine oxide using a room-temperature ionic liquid. *Science China Chemistry* 2014; 57: 1432–1438. doi: 10.1007/s11426-014-5194-8
7. Zhong L, He F, Liu Z, et al. Adsorption of uranium (VI) ions from aqueous solution by acrylic and diaminomaleonitrile modified cellulose. *Colloids and Surfaces A: Physicochemical and Engineering Aspects* 2022; 641: 128565. doi: 10.1016/j.colsurfa.2022.128565
8. Wu J, Tian K, Wang J. Adsorption of uranium (VI) by amidoxime modified multiwalled carbon nanotubes. *Progress in Nuclear Energy* 2018; 106: 79–86. doi: 10.1016/j.pnucene.2018.02.02
9. Bulgariu D, Nemeş L, Ahmed I, Bulgariu L. Isotherm and kinetic study of metal ions sorption on mustard waste biomass functionalized with polymeric thiocarbamate. *Polymers* 2023; 15(10): 2301. doi: 10.3390/polym15102301
10. Torkaman R, Maleki F, Gholami M. Assessing the radiation-induced graft polymeric adsorbents with emphasis on heavy metals removing: A systematic literature review. *Journal of Water Process Engineering* 2021; 44: 102371. doi: 10.1016/j.jwpe.2021.102371
11. Nazia R, Chandra DN, Shahnaz S, et al. Application of acrylic acid and sodium styrene sulfonate grafted non-woven PE fabric in methylene blue removal. *Research Journal of Chemistry and Environment* 2020; 24(5): 36–43.
12. Nasef MM. Gamma radiation-induced graft copolymerization of styrene onto poly(ethyleneterephthalate) films. *Journal of Applied Polymer Science* 2000; 77(5): 1003–1012. doi: 10.1002/1097-4628(20000801)77

13. Agarwal M, Singh K. Heavy metal removal from wastewater using various adsorbents: A review. *Journal of Water Reuse and Desalination* 2017; 7(4): 387–419. doi:10.2166/wrd.2016.104
14. Shao D, Li Y, Wang X, et al. Phosphate-functionalized polyethylene with high adsorption of uranium (VI). *ACS Omega* 2017; 2(7): 3267–3275. doi: 10.1021/acsomega.7b00375
15. Rahman N, Sato N, Yoshioka S, et al. Selective Cu (II) adsorption from aqueous solutions including Cu (II), Co (II), and Ni (II) by modified acrylic acid grafted PET film. *International Scholarly Research Notices* 2013; 2013. doi: 10.1155/2013/536314
16. Zu J, Tang F, He L, et al. Facile synthesis and properties of a cation exchange membrane with bifunctional groups prepared by pre-irradiation graft copolymerization. *RSC Advances* 2018; 8: 25966–25973. doi: 10.1039/C8RA03472A
17. Sithambaranathan P, Nasef MM, Ahmad A, et al. Composite proton-conducting membrane with enhanced phosphoric acid doping of basic films radiochemically grafted with binary vinyl heterocyclic monomer mixtures. *Membranes* 2023; 13: 105. doi: 10.3390/membranes13010105
18. Atia KS, El-Arnaouty MB, Ismail SA, et al. Characterization and application of immobilized lipase enzyme on different radiation grafted polymeric films: Assessment of the immobilization process using spectroscopic analysis. *Journal of Applied Polymer Science* 2003; 90: 155–167. doi: 10.1002/app.12620
19. Nasef M, Saidi M, Ahmad H, et al. Optimization and kinetics of phosphoric acid doping of poly(1-vinylimidazole)-graft-poly(ethylene-co-tetrafluoroethylene) proton conducting membrane precursors. *Journal of Membrane Science* 2013; 446: 422–432. doi: 10.1016/j.memsci.2013.05.053
20. González-Blanco C, Rodríguez LJ, Velázquez MM. Effect of the addition of water-soluble polymers on the structure of aerosol OT water-in-oil microemulsions: A Fourier Transform Infrared spectroscopy study. *Langmuir* 1997; 13(7): 1938–1945. doi: 10.1021/la960451q
21. Nasefa MM, Saidi H, Dahlan KZM. Single-step radiation induced grafting for preparation of proton exchange membranes for fuel cell. *Journal of Membrane Science* 2009; 339(1–2): 115–119. doi: 10.1016/j.memsci.2009.04.037
22. Khedr RF. Synthesis of amidoxime adsorbent by radiation-induced grafting of acrylonitrile/acrylic acid on polyethylene film and its application in Pb removal. *Polymers* 2022; 14(15): 3136–3157. doi: 10.3390/polym14153136
23. Calleja G, Houdayer A, Etienne-Calas S, et al. Conversion of poly (ethylene-alt-tetrafluoroethylene) copolymers into poly(tetrafluoroethylene) by direct fluorination: A convenient approach to access new properties at the ETFE surface. *Journal of Polymer Science Part A: Polymer Chemistry* 2011; 49(7): 1517–1527. doi: 10.1002/pola.24588
24. Alswata AA, Ahmad MB, Al-Hada NM, et al. Preparation of zeolite/zinc oxidenano composites for toxic metals removal from water. *Results Physics* 2017; 7: 723–731. doi: 10.1016/j.rinp.2017.01.036
25. Sayed EME, Tamer TM, Omer AM, et al. Development of novel chitosan schiff base derivatives for cationic dye removal: Methyl orange model. *Desalination and Water Treatment* 2016; 57(47): 22632–22645. doi: 10.1080/19443994.2015.1136694
26. Yang Z, Chai Y, Zeng L, et al. Efficient removal of copper ion from wastewater using a stable chitosan gel material. *Molecules* 2019; 24(23): 4205–4219. doi: 10.3390/molecules24234205
27. Massai H, Raphael D, Sali M. Adsorption of copper ions (Cu⁺⁺) in aqueous solution using activated carbon and biosorbent from Indian jujube (*Ziziphus mauritiana*) seed hulls. *Chemical Science International Journal* 2020; 29: 13–24. doi: 10.9734/CSJI/2020/v29i530177
28. Tahir M, Raza A, Nasir A, et al. Radiation induced graft polymerization of glycidyl methacrylate onto sepiolite. *Radiation Physics and Chemistry* 2021; 179: 109259. doi: 10.1016/j.radphyschem.2020.109259
29. Kamal A, Bibi S, Bokhari SW, et al. Synthesis and adsorptive characteristics of novel chitosan/graphene oxide nanocomposite for dye uptake. *Reactive and Functional Polymers* 2017; 110: 21–29. doi: 10.1016/j.reactfunctpolym.2016.11.002
30. Rahman N, Biswas MI, Kabir M, et al. Pre-irradiation grafting of acrylic acid and sodium styrene sulfonate on non-woven polyethylene fabric for heavy metal removal. *Environmental Research & Technology* 2021; 4(1): 63–72. doi: 10.35208/ert.828089
31. Yadav SK, Dixit AK. Efficient removal of Cr(VI) from aqueous solution onto palm trunk charcoal: Kinetic and equilibrium studies. *Chemical Sciences Journal* 2015; 7(1): 1–7. doi: 10.4172/2150-3494.1000114
32. Sardar MN, Rahman N, Sultana S. Application of radiation grafted waste polypropylene fabric for the effective removal of Cu (II) and Cr (III) ions. *Journal of Polymer Engineering* 2022; 42(5): 266–276. doi: 10.1515/polyeng-2021-0177
33. Maheshwari U, Mathesan B, Gupta S. Efficient adsorbent for simultaneous removal of Cu(II), Zn(II) and Cr(VI): Kinetic, thermodynamics and mass transfer mechanism. *Process Safety Environmental Protection* 2015; 98: 198–210. doi: 10.1016/j.psep.2015.07.010
34. Milicevic S, Boljanac T, Martinovic S. Removal of copper from aqueous solutions by low cost adsorbent-Kolubara lignite. *Fuel Processing Technology* 2012; 95: 1–7. doi: 10.1016/j.fuproc.2011.11.005

35. Yavuz O, Altunkaynak Y, Guze F. Removal of copper, nickel, cobalt and manganese from aqueous solution by kaolinite. *Water Research* 2003; 37(4): 948–952. doi: 10.1016/S0043-1354(02)00409-8
36. Li N, Bai R. Copper adsorption on chitosan-cellulose hydrogel beads: Behaviors and mechanisms. *Separation and Purification Technology* 2005; 42(3): 237–247. doi: 10.1016/j.seppur.2004.08.002
37. Eloussaief M, Jarraya I, Benzina M. Adsorption of copper ions on two clays from Tunisia: pH and temperature effects. *Applied Clay Science* 2009; 46(4): 409–413. doi: 10.1016/j.clay.2009.10.008
38. Kumar PS, Subramaniam R, Vasanthakumar S, et al. Removal of copper(II) ions from aqueous solution by adsorption using cashew nut shell. *Desalination* 2011; 266(1–3): 63–71. doi: 10.1016/j.desal.2010.08.003
39. Bsoul AA, Zeatounb L, Abdelhayc A. Adsorption of copper ions from water by different types of natural seed materials. *Desalination and Water Treatment* 2014; 52(31–33): 5876–5882. doi: 10.1080/19443994.2013.808593
40. Peng X, Li Y, Liu S, et al. A study of adsorption behaviour of Cu(II) on hydroxyapatite-coated-limestone/chitosan composite. *Journal of Polymers and the Environment* 2021; 29: 1727–1741. doi: 10.1007/s10924-020-02009-x
41. Peng X, Chen W, He Z, et al. Removal of Cu(II) from wastewater using doped HAP-coated-limestone. *Journal of Molecular Liquids* 2019; 293: 111502–111511. doi: 10.1016/j.molliq.2019.111502
42. Dan Li, Feigao Xu. Removal of Cu (II) from aqueous solutions using ZIF-8@GO composites. *Journal of Solid State Chemistry* 2021; 302: 122406. doi: 10.1016/j.jssc.2021.122406